Journal of Sol-Gel Science and Technology

Glycerol etherification towards selective diglycerol over mixed oxides derived from hydrotalcites: Effect of Ni loading

--Manuscript Draft--

Manuscript Number:	JSST-D-20-00044
Full Title:	Glycerol etherification towards selective diglycerol over mixed oxides derived from hydrotalcites: Effect of Ni loading
Article Type:	Original Paper
Keywords:	Mixed oxides; hydrotalcite; etherification; glycerol; di-glycerol.
Abstract:	A series of tetrametallic hydrotalcite with different Ni loading, were synthesized by coprecipitation method. The effect of Ni loading on the structural and textural features was investigated by various techniques such as X-ray diffraction (XRD), thermogravimetric analysis TG-DSC-MS, temperature programmed reduction (H 2 -TPR), temperature programmed desorption (NH 3 -TPD) and 1-butene isomerization as a model reaction to probe acid-base character of catalysts. Mixed oxides derived from hydrotalcites are found to be active and suitable, via solvent free, in the glycerol etherification reaction. A gradual enhance of glycerol conversion is revealed when increasing the Ni/Mg molar ratio and the most active catalyst found is HTc-Ni 75% with full selectivity to diglycerol.
Additional Information:	
Question	**Response**

Graphical Abstract

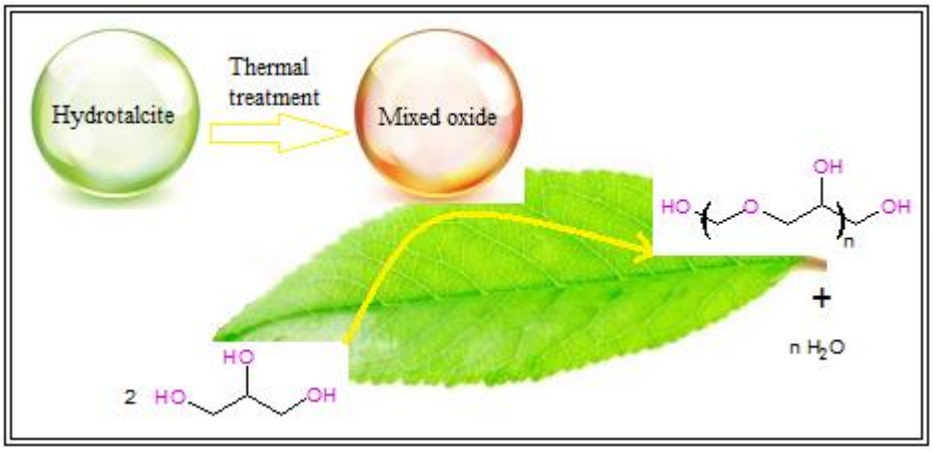

Declaration of interests

☒ The authors declare that they have no known competing financial interests or personal relationships that could have appeared to influence the work reported in this paper.

☒The authors declare the following financial interests/personal relationships which may be considered as potential competing interests:

Glycerol etherification towards selective diglycerol over mixed oxides derived from hydrotalcites: Effect of Ni loading

M. Aloui[a], J.A. Cecilia[b], R. Moreno-Tost[b], S.B. Ghorbel[a], M. Saïd Zina[a], E. Rodríguez-Castellón[b]

[a]Laboratoire de Chimie des Matériaux et Catalyse, Faculté des sciences de Tunis, Université de Tunis El Manar, 2092, Tunisia.
[b]Departamento de Química Inorgánica, Cristalografía y Mineralogía. Facultad de Ciencias. Universidad de Málaga. Campus de Teatinos 29071 Málaga (España).

Abstract

A series of tetrametallic hydrotalcite with different Ni loading, were synthesized by coprecipitation method. The effect of Ni loading on the structural and textural features was investigated by various techniques such as X-ray diffraction (XRD), thermogravimetric analysis TG-DSC-MS, temperature programmed reduction (H_2-TPR), temperature programmed desorption (NH_3-TPD) and 1-butene isomerization as a model reaction to probe acid-base character of catalysts. Mixed oxides derived from hydrotalcites are found to be active and suitable, via solvent free, in the glycerol etherification reaction. A gradual enhance of glycerol conversion is revealed when increasing the Ni/Mg molar ratio and the most active catalyst found is HTc-$Ni_{75\%}$ with full selectivity to diglycerol.

Keywords: Mixed oxides, hydrotalcite, etherification, glycerol, di-glycerol.

Introduction

Currently, the production of biodiesel by transesterification of vegetable oils is in continuous growing, being glycerol the main by-product generated in this process with roughly 10wt% [1]. This surplus induces a significant drop of the glycerol prices making it widely valuable as a starting material for chemical production, hence it is useful in a large panel of applications including selective oxidation [2], hydrogenolysis to propanediol [3], dehydration to acrolein [4, 5], pyrolysis [6], transesterification [7] and etherification reaction [8]. Among these reactions, one of the most interesting and viable uses is the direct etherification of glycerol into polyglycerols by reacting glycerol with itself in presence of a basic catalyst and without solvent. Polyglycerols have an enormous potential in wide variety of fields such as polymers, cosmetics, food, dispersants, pharmaceutical industries, lubricants, biomedical or drug delivery systems [9-12]. Polyglycerols can be obtained from different synthetic strategies involving allylic ethers, incorporation of protective groups, via glycidol or epichlorohydrin intermediates; however the solventless catalytic etherification is more attractive as a result of environmental concerns [13].

The conversion of glycerol to reach desired short-chain polyglycerol remains a scientific challenge, in this sense the design of suitable catalysts to control the selectivity to specific products is highly desired [14]. Several researches have been focused on the use of basic homogeneous catalysts like hydroxides, carbonates and oxides [15,16] as well as acidic homogeneous catalysts [17,18] (such as sulfuric, benzene-sulfonic and dodecyl benzene-sulfonic acids). In fact, these catalysts recognize a high solubility in glycerol and/or a non-selective oligomerization because of the generation of high molecular weight glycerol oligomers coupled to others by-products through dehydration reaction, which is not promising industrially since it involves difficult and costly product separation and purification [19]. Thus, the attention has been shifted to the use of heterogeneous catalysts which are easily recovered, more suitable and selective for short chain polyglycerol.

Ruppert et al [20] investigated the use of alkaline earth metal oxides, like MgO, CaO, SrO and BaO. These authors pointed out that glycerol conversion is directly related to the amount and strength of the basic sites, reaching a high glycerol conversion around 60%, with selectivity to di- and triglycerol higher than 90%. However, alkaline earth oxides suffer from partial hydroxylation by water formed in the etherification reaction, making them instable at high temperature reaction (220-260°C). Ayoub et al [21] studied montmorillonite K-10 with

intercalated LiOH for selective production of diglycerol via solvent free glycerol etherification reaction. They found diglycerol selectivity about 53% and glycerol conversion around 98%. From experimental and theoretical studies, it has been reported that basic sites are involved in the glycerol etherification reactions but the Lewis acid sites also have a clear influence on the catalytic activity [20,22] , which has been confirmed by various authors [8,13,23]. In fact, solid acid catalysts such as ionic exchange resins [24,25], zeolites [24], clay minerals [21,26] or mesoporous silicas (SBA-15 and MCM-41) modified with aluminum species into the framework [23] have shown to be active in glycerol etherification reaction. However, this acidity must be controlled since a high amount of active sites causes an unwanted excessive polymerization [27].

Layered double hydroxides (LDHs), also named hydrotalcites (HTs) can be represented by the general formulae $[M^{2+}_{1-x}M^{3+}_{x}(OH)_2]^{x+}[A^{n-}_{x/n}]^{x-} \cdot mH_2O$, where M^{2+} (Mg^{2+}, Cu^{2+}, Zn^{2+}, Ni^{2+}) are divalent cations and M^{3+} (Al^{3+},Fe^{3+},Cr^{3+}) which form positively charged layers, which are counterbalanced with A^{n-} anions (CO_3^{2-}, NO_3^{-}, PO_4^{3-}) that are located in the interlayer spacing, while x the number of interlayer water molecules. LDHs are very promising materials in several fields such as adsorbent material or in catalysis. The calcination of LDHs between 450-600 ºC leads to formation of mixed oxides with Lewis basic sites [28,29]. In addition, the rehydration of the mixed oxides can recover the layered structured with the incorporation of hydroxyl anions in the interlayer region forming higher proportion of Brönsted basic sites [30]. The use of LDHs as catalytic precursor has a high potential to replace the homogenous-based catalysts since they are easy to prepare, relatively inexpensive catalysts, environmentally benign and recyclable [31]. The mixed oxides coming from LDHs have shown to be active in several organic reactions such as Claisen-Schmidt condensation [32,33], Michael addition [34], Knoevenagel condensation [35], or biodiesel transesterification [36,37].

Recently, the mixed oxides obtained from thermal treatment for the LDHs have been used as promising catalysts in the etherification reaction. Thus, Garcia-Sancho et al., have evaluated the influence of the type of precipitant agent, the calcination temperature in the specific surface area and the dispersion of MgO-Al_2O_3 species for the glycerol etherification to obtain polyglycerols [38]. On the other hand, Pérez-Barrado et al [8] have analyzed the influence of the acid-base properties of calcined MgAl and CaAl layered double hydroxide to obtain short-chain polyglycerols. Lately, Guerrero-Urbaneja et al [39] have optimized the Mg/Fe molar ratio of the LDHs to obtain short chain polyglycerols, reaching a conversion around 25% with diglycerol selectivity higher than 90 % in all cases. The acid and basic sites of the metal mixed

oxides formed upon calcination of LDHs are associated to the presence of O^{2-}-M^{n+} acid-base pairs. The nature, amount and strength of these sites depend on the preparation method, calcination temperature and the metal cations used in the synthetic step [40]. In addition, LDHs have been synthesized with a wide variety of mono- (Cu^{+}) [41] and tetravalent metal cations (Zr^{4+}) [42,43] to be used as catalytic precursor since these modifications improve the physicochemical properties of the final catalysts.

The present research modifies the acid-base properties of the metal mixed oxide coming from LDHs by a substitution of Al species by Zr species. Previous research has pointed out that metal mixed oxide obtained by calcining MgAl-LDH display high proportion of Lewis acid sites on its surface, which can be attributed to the presence of Al^{3+} species. The modification of Al^{3+} by other species with Lewis sites, such as Zr^{4+} can affect to the nature, amount and strength of these acid sites. On the other hand, the Lewis basicity of the Mg^{2+} species can be modified by the substitution of these Mg^{2+} by Ni^{2+} species. Thus, the aim of this research is the synthesis of Mg/Ni/Al/Zr HTs with different Ni loading by coprecipitation method in order to improve their catalytic properties for the target reaction. Structural and textural features of mixed oxide derived from hydrotalcite with different Ni loadings were studied and catalytic performances of all mixed oxides were evaluated in the glycerol etherification reaction.

2. Experimental

2.1 Chemicals

Precursor salt used in this work to synthesize the LDHs were magnesium nitrate hexahydrate, $Mg(NO_3)_2$ $6H_2O$ (>98%, Sigma-Aldrich), aluminum nitrate nonahydrate, $Al(NO_3)_2$ $9H_2O$ (>98%, Sigma-Aldrich), zirconium oxynitrate hydrate, $ZrO(NO_3)_2$ H_2O (99%, Sigma-Aldrich) and nickel nitrate hexahydrate $Ni(NO_3)_2$ $6H_2O$ (>98%, Sigma-Aldrich). Sodium hydroxide, NaOH (99%, Sigma-Aldrich) and sodium carbonate Na_2CO_3 (99.5%, Normapur) were used as precipitating agents. Finally, glycerol (98%, Sigma-Aldrich) was used as fed for the etherification reaction.

2.2 Catalysts preparation

Hydrotalcite-like compounds, were synthesized at room temperature by coprecipitation method at low supersaturation where M^{2+}/ (Al^{3+}+Zr^{4+}) global ratio was kept at 2, Al^{3+}+Zr^{4+} was fixed to 0.33 in all cases whereas Ni^{2+}/M^{2+} molar ratio was varied from 25 until 100 %. In order to

synthesize the LDHs, a basic solution of NaOH (2M) and Na_2CO_3 (0.5M) was mixed with an aqueous solution of metal salts under vigorous stirring at a constant pH (10 $\pm$0.1). The resulting precipitate was aged at 60 °C for 18 h then the solid was filtered, washed with distilled water until a neutral pH and dried in the oven at 80 °C. All catalysts were activated in a tubular furnace at 450 °C during 15 h, under a helium flow to obtain the derived mixed oxide.

Mixed oxides with different nickel loads were designated as follow: HTc-$Ni_{25\%}$, HTc-$Ni_{50\%}$, HTc-$Ni_{75\%}$ and HTc-$Ni_{100\%}$, where 25, 50, 75 and 100 % indicates the Ni^{2+} content in wt.% of the M^{2+} species.

2.3 Samples characterization

Powder diffraction patterns were collected on an PANalytical automated diffractometer, EMPYREAN model, using Cu-Kα_1,2 (1.5406 Å) radiation and a last generation PIXcel detector. The database employed were ICSD, PDF 2-2004 and COD of High ScorePlus programme of PANalytical.

TG–DSC was performed using a thermal Analyzer from METTLER TOLEDO model TGA / DSC 1. Analysis were performed in Al_2O_3 crucible 70 µl in the temperature range 30-900 °C, with nitrogen flow (50 ml / min) and a heating rate of 10°C min^{-1}. The equipment was coupled to a PFEIFFER VACUUM ThermoStar TM GSD 320 model mass spectrometer. The mass ratio measurement range was varied from 1 to 200. It consists of a Faraday detector and a SEM detector. The capillary was made in quartz and was operated at 200 ºC. The scanning speed was 2-60 uma / s, depending on the type of scan performed. The vacuum with a working pressure in the order of 10^{-6} mbar is achieved by a membrane pump and a turbo.

The textural parameters were determined from the N_2 adsorption–desorption isotherms at -196 ºC, obtained by using an automatic ASAP 2020 model of gas adsorption analyzer supplied for Micromeritics. Prior to N_2 adsorption, the sample were evacuated at 450 ºC (heating rate 10 ºC min-1) for 18 h. Surface areas were determined by using the Brunauer-Emmet-Teller (BET) equation, considered a N_2 molecule cross section of 16.2 $Å^2$ [44]. The total pore volume was calculated from the adsorption isotherm at P/P_0=0.996. The Density Functional Theory method (DFT) was employed to determine the pore size distribution [45].

The acidity of catalyst was determined by temperature programmed desorption of ammonia (NH_3-TPD). In each experiment, 80 mg of the calcined LDH were activated from room

temperature to 550 ºC in He flow (35 ml min^{-1}), maintaining the temperature 2h. After that, the sample was cooled to 100 °C and exposed to pure NH_3 flow for 5 min. Later, the physisorbed-NH_3 was removed using He flow (35 ml min^{-1}) and then, the physisorbed ammonia was removed using a He flow (35 ml min^{-1}). Finally, the NH_3-TPD was carried out from 100 ºC to 550 ºC, maintaining this temperature for 15 min using similar He flow as carrier gas. The NH_3 desorbed was registered using a Thermal Conductivity Reactor (TCD).

The catalytic isomerization of 1-butene was performed in a tubular glass flow microreactor. 80 mg of calcined LHDs were pretreated for 2 h in a He flow at 450 ºC (30 ml min^{-1}), and experiments were carried out at 400 ºC temperature. Experiments were performed in a tubular glass flow microreactor at $\tau = 0.6\ g_{cat}\ g^{-1}{}_{1\text{-but}}\ h$, and the time on stream was 120 min. The reactant 1-butene and the reaction products were analyzed on-line in a gas chromatograph (Shimadzu GC-14B) equipped with a wide bore $KCl/AlCl_3$ column. For this reaction, the distribution of n-butene was close to the equilibrium point.

The basicity was studied by temperature-programmed desorption of CO_2. 100 mg of calcined LDH was pretreated under a He stream at 450 ºC for 2 h (2 ºC min^{-1}, 100 mL min^{-1}). Then, the sample was cooled until 100 ºC, and a flow of pure CO_2 (50 mL min^{-1}) was subsequently introduced into the reactor during 1 h. The CO_2-TPD was carried out between 100 and 800 ºC under a helium flow (10 ºC min^{-1}, 30 mL min^{-1}), and evolved CO_2 was analyzed by an on-line with a TCD, after passing by an ice-NaCl trap to eliminate any trace of water.

The reducibility of Ni species was determined by H_2-thermoprogrammed reduction (H_2-TPR). 80 mg of calcined LDH were previously treated with a He flow (35 mL min^{-1}) at 450 ºC for 2 h. After cooling to room temperature, the H_2 consumption was studied between this temperature and 800 ºC, by using an Ar/H_2 flow (48 mL min^{-1}, 10 vol.% of H_2) and a heating rate of 10 °C min^{-1}. Water formed in the reduction process was removed with an isopropanol-liquid nitrogen trap and a cold finger (−80 ºC). The H_2 consumption was measured with an on-line TCD, and quantified by calibration with pure CuO as reference standard (Aldrich), assuming a total reduction of CuO to Cu^0.

X-ray photoelectron spectroscopy (XPS) studies were performed with a Physical Electronics PHI 5700 spectrometer equipped with a hemispherical electron analyzer (model 80-365B) and a Mg Kα (1253.6 eV) X-ray source. High-resolution spectra were recorded at 45° take-off-angle by a concentric hemispherical analyzer operating in the constant pass energy mode at 29.35 eV,

using a 720 μm diameter analysis area. Charge referencing was done against adventitious carbon (C 1*s* at 284.8 eV). The pressure in the analysis chamber was kept lower than 5×10^{-6} Pa. PHI ACCESS ESCA-V6.0 F software package was used for data acquisition and analysis. A Shirley-type background was subtracted from the signals. Recorded spectra were always fitted using Gauss-Lorentz curves in order to determine more accurately the binding energy of the different element core levels.

The leaching of the mixed oxides was evaluated by ICP-AES by using a Perkin Elmer (model ELAN DRC-e) spectrometer.

2.4 Reaction procedure

The catalytic activity was evaluated in the etherification of glycerol between 210-240 ºC in a three-necked glass batch reactor without solvent, equipped with a water-cooled condenser coupled with a Dean-Stark system to remove the formed water, thermometer and vigorous stirring. The atmosphere of the reactor was kept inert by means of a N_2 flow of 15 mL min^{-1}. Before the reaction, catalysts were activated at different temperatures for 15 h (heating rate, 2 ºC min^{-1}), under a helium flow. The reaction was stopped at 24 h and catalysts were separated by filtration on a porous plate. The reaction products were analyzed by means of gas chromatography. An aliquot (*ca* 80 mg) of the reaction mixture was dissolved in dried pyridine (Aldrich) and then N,O-bis(trimethylsilyl)trifluoroacetamide was added. This solution was aged in a stove at 60 ºC during 1 h and analyzed in a gas chromatograph (Shimadzu GC model 14A) equipped with FID and a capillary silica fused TBR-14 column (Teknochroma). The only detected products were unreacted glycerol, di- and tri-glycerol. The selectivities to the different products were calculated as the weight ratio of the respective product to the sum of products formed. The glycerol conversion was calculated as the ratio of the detected glycerol to the sum of the glycerol and products formed.

The detected products were unreacted glycerol, di- and tri-glycerols. The glycerol conversion was determined from (Eq. 1):

$$x_{Gly} = \frac{n_0 - n_f}{n_0} \times 100 \qquad (1)$$

where, n_0 is the initial amount of glycerol mol and n_f is the final amount of glycerol mol.

The Selectivity (S_{olig}) was calculated using (Eq. 2).

$$S_{olig} = \frac{n_{olig}}{n_0 - n_f} \times 100 \qquad (2)$$

where n_{olig} is the amount of each oligomer in mol.

Yields were calculated using (Eq. 3).

$$Y_{olig} = \frac{X_{Gly}\, \Sigma\, s_{olig}}{100} \qquad (3)$$

Oligoglycerols higher than triglycerol were not detected by this analytical procedure, so that other products not detected were labeled as others, which could include acrolein or glycidol among others.

3. Results and discussion

3.1. Catalyst characterization

3.1.1. Powder X-ray diffraction (PXRD)

The XRD patterns of the as-prepared hydrotalcites containing Ni with different Ni^{2+}/M^{2+} molar ratio are shown in Fig. 1. XRD data of the synthesized hydrotalcites displayed the typical reflections peaks of a well-crystallized HT (JCPDS file: 70-2151) belonging to the space group R 3m and related to the presence of the (003), (006) and (009) crystal planes in the layered structure. The diffractograms discard the segregation of phases of Zr^{4+} species, indicating that Zr^{4+} cations are incorporated into the structure or at least are well dispersed. In addition, the absence of diffraction peaks attributed to nickel species also indicates a good incorporation of Ni^{2+} cations into the brucite layers. The unit cell parameter, *a*, is the average distance between two metal ions within the layers, and it has been calculated from the *d*-spacing of the (110) reflection ($a = 2d_{110}$). The *c* parameter is three times the distance between adjacent hydroxide and it has been also calculated from the (003) reflection ($c = 3d_{003}$). The obtained values are very close to those reported by other authors [46,47] for hydrotalcites with carbonates in the interlayer space, which confirms that the incorporation of Ni^{2+} and Zr^{4+} species does not cause clear modifications in the lamellar structure of the hydrotalcites.

The increase of Ni content has led to the formation of wider diffractions peaks, which suggests a progressive loss of the crystallinity. Considering that both cations present similar ionic radii,

0.52 angstroms Mg^{2+} cation and 0.72 angstroms for Ni^{2+} cation, the isomorphic substitution can cause changes in the 2θ values of the diffractions peaks, being only noticeable a slight displacement at lower 2θ values only for the sample HT-$Ni_{100\%}$. The gradual modification in the width and intensity of the diffraction peaks when Mg^{2+} is replaced by Ni^{2+} species could be attributed to both cations precipitate at different pH values, which can affect the self-assembly of the lamellar structure. The crystal size was estimated by the Rietveld method, obtaining crystals with a size lower than 5 nm. In fact, the progressive substitution of Mg^{2+} by Ni^{2+} in the synthetic step causes a slight decrease in the crystal size.

3.1.2 TG/DSC analysis and evolved CO_2

In order to determinate the optimum calcination temperature of the LDHs Thermogravimetric (TG) and Differential Scanning Calorimetry (DSC) curves as well as the evolved CO_2 followed by mass spectroscopy (m/z=44) were investigated. From TG curves (Figure 2A), two main typical regions are observed. The first region occurred bellow 250°C, corresponding to the loss of physisorbed and interlayer water with no significant influence on the HT-lamellar structure. Otherwise the second region arise between 250 and 800°C, related to the dehydroxylation of the brucite sheets by water removal and decarboxylation by decomposition of carbonate ions, resulting in the collapse of the layer structure and the formation of carbon dioxide. In addition, it is known that the thermal stability of HTs depends on the nature of the layer cations and interlayer anions, comparing the TG/DSC curves of all samples (Figure 2B), it is found that the variation of Ni content led to some changes in the thermal stability of these compounds. Both TG and DSC analysis reveals that LDHs with lower nickel content loss higher proportion of physisorbed and interlayer water.

With regard to the second step, DSC analysis reveals as Ni loading was increased the temperature of this second diminished. This fact was confirmed following the CO_2 emission signal (m/z=44) as illustrated in Figure 3, where the maximum value is shifted from 375 ºC for HT-$Ni_{25\%}$ to 320 ºC for HT-$Ni_{100\%}$, which could be related to a slight decrease of the crystallinity for higher Ni content and with a lower interaction between the brucite layer with the CO_3^{2-} species used to counterbalance the charge deficiency. Considering the DSC analysis, each LDH was calcined at 450 ºC for 2 h to obtain the corresponding mixed oxide.

The thermal treatment under helium flow leads to the destruction of the hydrotalcite structure with remarkable structural changes and the formation of mixed oxide phase. The diffraction patterns (Fig. 4) of all mixed oxides are similar and present low crystallinity with broad peaks.

The main peaks characteristic of hydrotalcite structure disappeared, and new diffraction peaks appeared about 36, 42 and 63°. Taking into account that these diffractions peaks could be ascribed to NiO or MgO species, it is impossible to discern between both phases since both phases display the same packaging and similar ionic radius (Mg^{2+}=65 pm and Ni^{2+}=69 pm) so the diffraction peaks of each phase are very close so it is not possible to determine the size of the crystal. However, the diffraction peak at 2θ = 36º increases the intensity as the Ni loading does. This issue could indicate about some segregation of NiO. In any case, the diffraction peaks of the mixed oxides are very broad, suggesting the presence of a small particle size and high dispersion. The XRD profiles of the calcined samples do not reflect the existence of diffraction peaks attributed to Al_2O_3 or ZrO_2 in any case, confirming both the low crystallinity of these oxides and the incorporation of Al^{3+} and Zr^{4+} in the structure of MgO.

3.1.3. TEM micrograph

The morphology of the LDHs thermally treated was evaluated by TEM (Figure 5). It is noteworthy that all micrographs display homogenous structures, discarding the formation of segregated species with higher particle size, as was suggested by XRD (Figure 2B). TEM micrographs show that the mixed oxide particles are formed by aggregates of small structures with laminar or fibrous forms. In addition, it is noteworthy that an increase of the nickel content led to the formation of smaller aggregates.

3.1.4. Physisorption of N_2 at -196 ºC

The textural properties of mixed oxides obtained by thermal treatment of LDHs were determined from the N_2 adsorption-desorption at -196 ºC (Figure 4). According to the IUPAC classification, all isotherms can be considered as type-II, which are typical of macroporous materials [48], as indicates the increase of the N_2 adsorbed at higher relative pressures. Taking into account that the mixed oxides itself lack porosity, the specific surface area S_{BET} is attributed to the N_2-filled in the space between the small layers. In any case, all oxides showed similar S_{BET} values from 194 m^2/g to 227 m^2/g, which means a high dispersion of these mixed oxides. The hysteresis loop can be adjusted to type H3 hysteresis for all calcined hydrotalcites, which is usually found in materials consisting of aggregates of particles forming slit-shaped pores with non-uniform size or shape [48].

3.1.5. Reducibility and reduction temperature of catalysts

The study of the reducibility of nickel species was investigated to evaluate how the dispersion or the interaction with other oxide species changes when the nickel loading is modified. The data shown in Figure 7 reveal that the reduction of all mixed oxides takes place in a step, could be assigned to the reduction of Ni^{2+} species from mixed oxide to Ni^0, in the range 300-900°C. However, the width of this peak reveals the existence of different Ni^{2+} species interacting with different metals. It seems that as Mg^{2+} loading is decreased (i.e. the Ni^{2+} is increased) the H_2-consumption takes place at lower temperature, so the Ni-Mg interaction should be stronger, which is in agreement with the literature [49].

3.1.6. XPS results

In order to determinate the chemical composition of the mixed oxides, XPS measurements were carried out. The C 1*s* core level spectra display two contributions located at 284.8 eV and 289.4-289.7 eV, which are ascribed to the presence of adventitious carbon and carbonate species, respectively. In spite the thermal treatment at 450 ºC, it is noteworthy the existence of carbonate species. In this sense, previous authors have also detected carbonate species after the thermal treatment of the LDHs [39], being attributed to the remaining strong bonded carbonates and/or the recarbonation of the mixed oxides during the sample handling.

The O 1*s* core level spectra also show the coexistence of two bands located at 529.8-530.1 eV and 531.5-531.9 eV, which are assigned to the presence of O^{2-} and species like -OH or carbonates groups [39]. From the data obtained in Table 2, it can be observed that the concentrations of both contributions are similar in all cases, although the proportion of oxides species slightly increases in the case of HTc-$Ni_{100\%}$.

In the case of the Mg 2*p* core level spectra, it is only noteworthy the existence of a single contribution located between 49.5-49.9 eV, which is assigned to Mg^{2+} in an oxidic environment. It is also noticeable that the Mg content decreases according as Mg^{2+} species are replaced by Ni^{2+} ones, as was expected. The analysis of the theoretical Ni^{2+}/M^{2+} reveals that the obtained values are higher than the theoretical ones, which indicates an enrichment of the surface with Ni^{2+} for the mixed oxides. As Mg^{2+} and Ni^{2+} displays different ionic radii, the phase segregation cannot be discarded since the diffraction peaks of both phases appear at similar 2θ values. Thus, it is possible that a portion of Ni^{2+} can be within hydrotalcite structure and another portion is segregated, being located mainly on the surface, as indicates the atomic concentrations (Table 2). Both Al 2*p* and Zr 3*d* core level spectra showed an unique contribution located at 73.5-74.0

eV in the case of Al 2*p* region and 182.2-182.5 eV for the Zr 3*d* region, assigned in all cases to oxides species. With regard to the $Zr^{4+}/(Al^{3+}+Zr^{4+})$ ratio, the data shown in Table 2 report that those ratios are slightly lower than the theoretical value (0.33), indicating that Zr^{4+} are less exposed on the surface of the mixed oxides by a possible phase segregation. Finally, the $(Ni^{2+}+Mg^{2+})/(Al^{3+}+Zr^{4+})$ molar ratio is close to 2.00 in all samples, which is in agreement with the theoretical data, except in HTc-$Ni_{100\%}$ where the proportion of M^{2+} species is higher on the surface because of the segregation of NiO and Al_2O_3 phases.

3.1.7. Acid-base properties

As was indicated previously, both acid and basic sites are involved in the etherification reactions so the quantification of these active sites may become a key parameter in the evaluation of the catalytic behavior.

The amount and strength of acid sites in calcined hydrotalcites were investigated by temperature programmed desorption of ammonia (NH_3-TPD). The NH_3-TPD profiles of all calcined HTs (Fig. 8) show a broad asymmetrical shape indicating the presence of acid sites showing different strengths. Previously, some authors have considered the deconvolution of the NH_3-TPD profile in three desorption sites [50]. Weak acid sites occurred at temperature below 200 °C, moderate acid sites located in the temperature range of 200-350°C and strong acid sites strength associated to temperatures above 350°C.

As the Ni^{2+} loading some effects are observed from the TPD-NH_3 plots. First, the HTc-$Ni_{100\%}$ only shows a broad band of desorption of ammonia, leading to only the presence of weak-moderate of acid strength. When Mg and Ni are both present in the hydrotalcite, the mixed oxides display two visible bands. The band at low temperature decreases the intensity as the Ni loading increases and the band at higher temperature is shifted to lower temperatures as the Ni/Mg ratio increases. Taking into account that all the solids present the same amounts of Al and Zr, these features could be ascribed to the relationship between Ni and Mg. The cationic radii of Ni is 0.72 angstroms and the corresponding to Mg is 0.52 angstroms, this could imply that when the Ni loading is low it could be incorporated to the periclase structure and therefore it is well dispersed and it generates Lewis acid sites with moderate-strong strength of acid sites and as Ni/Mg ratio is increased this peak decreases the intensity and is shifted to lower temperatures. So, this peak could be ascribed to acidic Ni^{2+} species. Also, the peak at low

temperature is lowered its intensity as Ni/Mg increases, therefore those acid sites could be ascribed to Mg^{2+} species.

Shen et al [51] admitted the presence of both Brønsted and Lewis acid site in HTs calcined in similar temperature range. Brønsted sites are related to surface protons and are weaker than Lewis sites, which are associated with Al^{3+} cations located in octahedral sites [52]. The incorporation of Zr^{4+} cations in the synthetic step also provides Lewis sites [53]. In any case, the presence of H_2O as by-product in the etherification reaction can convert the Lewis acid sites to Brønsted sites, as was indicated by other authors previously [53,54]. The total numbers of acid sites of catalysts, illustrated in Table 3, reveals that HTc-$Ni_{75\%}$ is the sample with the highest amount of total acid sites in comparison with others catalysts.

In spite that all catalysts were prepared with the same loading of Al^{3+} and Zr^{4+}, the profiles differ among them. Thus, it is clear that the strength of the acid sites diminishes according as nickel content increases. The textural parameters of the calcined hydrotalcites hardly suffered modification in their S_{BET} values so the amount of available sites should be similar in all cases. In this sense, Ruppert et al. have pointed out that alkaline metal oxides can coordinate unsaturated metal cations acting as Lewis sites [20], which can generate strong acid sites [52] which can increase the activity of the active phase in the glycerol etherification.

As was indicated previously, the NH_3-TPD is an appropriate technique to evaluate the strength and amount of acid sites; however, it is impossible to discern between acid and basic sites. 1-Butene isomerization reaction is considered a model reaction to the acidity of these calcined hydrotalcites [55,56]. This reaction proceeds by acid centers and takes place through a first step where the C=C bond is shifted, obtaining cis- and trans- 2-butene, as products. In a second step, the isomerization to obtain isobutene takes place, although this step requires the presence of stronger acid sites. The use of catalysts with amount and strong acid sites can cause the cracking reactions with the formation of C2, C3, C5, and C6 olefins, the dimerization to octanes or even the formation of carbonaceous deposits. 1-butene isomerization is an interesting reaction since the type of acidity and the strength of the active sites affect the selectivity strongly. There are two types of isomerization. The double bond isomerization does not require very strong acidity. In this case, the cis/trans- 2-butenes ratio provides insights into the acid (cis/trans < 1) or basic (cis/trans > 1) nature of the catalyst. The other isomerization reaction is attributed to methyl shift, which only proceeds in strong sites. The dehydrogenation of 1-butene is directly related

with the Ni content. In this sense, previous research has reported that NiO-based catalysts favor the dehydrogenation reactions [57].

The data shown in Table 4 reveal that the conversion in the 1-butene isomerization reaction is relatively low (between 31.6 and 46.3 %) for the mixed oxides Mg-Ni. This value decreases in the case of calcined hydrotalcite without Mg, which only reaches a conversion value of 6.1 %. With regard to the selectivity, both cis- and trans-2-butene are the main products in all cases. The analysis of the cis-/trans-2-butene ratio reveals values above than one in all cases, which confirms the basic nature of the catalyst. The selectivity towards isobutene and 1,3-butadiene defines the strength of the acid sites [55,56]. Data shown in Table 3 indicate that HTc-$Ni_{25\%}$, HTc-$Ni_{50\%}$ and HTc-$Ni_{75\%}$ exhibit a low proportion of acid sites with high strength. In the case of HTc-$Ni_{100\%}$, the activity in the 1-butene isomerization is lower, although the selectivity to isobutene and 1,3-butadiene is slightly higher, which supposes low proportion of acid sites than those calcined hydrotalcites containing magnesium.

The amount and strength of the basic sites were determined by CO_2-TPD (Figure 9). In all cases, it can be observed the presence of two well defined bands, which indicates the existence basic sites with different strength. Previous research have reported that the first CO_2 desorption located at lower temperature, in the range of 100-300 ºC, is attributed to the desorption of bicarbonate formed on weakly OH groups, while the second broad CO_2 desorption band, which takes place between 450-700 ºC, is related with the unidentaded carbonated basic formed with surface O^{2-} ions [58,59]. CO_2 desorption data, shown in Figure 9, reveal that the desorption located at higher temperature decreases according as Mg^{2+} are substituted by Ni^{2+}, and also is shifted to lower desorption temperatures while the desorption located at lower temperature is maintained. These data suggest that Mg^{2+} provides the stronger basic sites, while the basicity attributed to NiO must be weaker.

3.2 Catalytic activity

3.2.1. Performance of Ni/Mg molar ratio on the catalytic activity

The HTc-Ni mixed oxides with different Ni loading were investigated in glycerol etherification using a batch reactor between 210-240 ºC, at atmospheric pressure under N_2 atmosphere.

In a preliminary test, the thermal contribution was evaluated in the glycerol etherification reaction in absence of catalyst (Figure 10). The catalytic data after 24 h at 220 ºC show a glycerol conversion of only 10% with a diglycerol selectivity of 93%. With regard to the mixed oxides, all samples are active for the etherification reaction of glycerol with full selectivity towards diglycerol. The catalytic data reveals that a gradual enhance of the diglycerol yield from 29% for HTc-$Ni_{25\%}$ to 55% for HTc-$Ni_{75\%}$. A commercial hydrotalcite, supplied by Aldrich, was calcined and used as reference in the synthesis of polyglycerols using similar catalytic conditions, reaching a glycerol conversion of 21 %, being only detected diglycerols. The data also were compared with the MgO prepared by activation of the corresponding nitrate at 700 ºC, obtaining a glycerol conversion of 31% with a diglycerol selectivity of 90% [22], while the Al_2O_3 synthesized by similar synthetic procedure only reaches a diglycerol yield close to 10%.

The catalytic data, shown in Fig.10, indicates that the presence of Ni^{2+} species has a positive effect in the catalytic behavior of the glycerol etherification. In this sense, previous research pointed out that the incorporation of Ni^{2+} also caused an improvement of the catalytic behavior in basic reactions such as the glycerol carbonate synthesis by the presence of basic sites with variable strength [60]. It is well reported in the literature that the glycerol etherification is a reaction that implies both basic and Lewis acid sites [20,22]. Data reported in Tables 3-4 and Fig.8 show how the catalytic behavior follows similar trend to NH_3-TPD and 1-butene isomerization from the HTc-$Ni_{25\%}$ to HTc-$Ni_{75\%}$. In the case of the HTc-$Ni_{100\%}$ the amount of the acid sites diminishes along with the conversion of 1-butene. With regard to the basic sites determined by CO_2-TPD, it can be observed that the amount of basic sites decreased for the HTc-$Ni_{100\%}$, mainly by the absence of stronger basic sites. The decrease of the amount both acid and basic sites can be related with the lower glycerol conversion in the HTc-$Ni_{100\%}$ catalyst.

In all cases, the conversion values are lower than those obtained using Na_2CO_3 as catalyst, which reaches a total conversion of 100 % after 24 h of reaction [61]. In this sense, some authors have previously pointed out that the carbonate of alkaline metals show the highest glycerol conversion due to the solubility of such carbonates in the glycerol however these homogenous catalysts are poor selective to dyglicerol [38,61]. Nonetheless, the use of heterogeneous catalysts also display some advantages related to the easier separation of the catalyst and the reusability of the catalyst.

It is difficult to carry out a comparison between the catalytic data previously reported in the literature with those shown in the present research. Ruppert et al. evaluated the catalytic behavior of different alkaline-earth metal oxides (MgO, CaO, SrO and BaO) establishing that the catalytic activity is directly related with the strength of basic sites [20]. The use of catalysts with strong basic sites causes the uncontrolled polymerization of the glycerol. Barros et al., evaluated the catalytic activity of the calcined eggshell (CaO) under similar catalytic conditions, reaching higher conversion values [58], although the selectivity towards diglicerols is lower due to the stronger basic sites. In order to diminish the strength of the basic sites and to increase the amount of available acid sites, MgAl hydrotalcites were synthesized and then calcined to obtain the mixed oxides [38]. These mixed oxides reached a highest conversion value of 50.7% with selectivity towards diglycerols of 84.8% under similar reaction conditions, were used in this study [38]. In the same way, these authors also synthesized MgFe-O mixed oxides from hydrotalcites as active phase in the glycerol etherification obtaining a glycerol conversion of 41% with selectivity close to 90% [39]. Considering the catalytic data reported in the literature using similar reaction conditions, it seems clear that both the incorporation of Ni^{2+} species into the hydrotalcite improve the glycerol conversion, obtaining diglycerols as unique product.

The mixed oxide that exhibited the highest conversion values and diglycerol yield, i.e. HTc-$Ni_{75\%}$, was chosen to optimize the reaction parameters in the glycerol etherification.

3.2.2. Influence of the catalyst loading

Firstly, the effect of the catalyst loading was evaluated on the glycerol etherification reaction at 220 ºC and 24 h (Fig. 11). Catalytic data reveals that the maximum conversion value is reached using only 2 wt.% of HTc-$Ni_{75\%}$ catalyst, achieving a glycerol conversion of 55% with a diglycerol selectivity of 100%. The increase of the catalyst content does not seem to be beneficial neither for glycerol conversion nor for diglycerol selectivity. Indeed, the use of a loading charge of 6 wt.% causes a significant decrease of the diglycerol selectivity to reach 54% along with the formation of triglycerol product ($S_{Triglycerol}$ = 46%). The use of larger amount of catalyst can cause diffusional problems limiting the glycerol conversion. On the other hand, other authors have established that the decrease of glycerol conversion may occur because of the back-scission of diglycerol to glycerol [62]. In addition, the use of larger amount of catalyst also causes an increment of the amount of acid and basic sites and therefore an increase of its reactivity, resulting in the reaction evolves beyond diglycerol molecule due to uncontrolled etherification.

3.2.3. Influence of the reaction temperature

The influence of the reaction temperature on the catalytic behavior of HTc-$Ni_{75\%}$ was another parameter evaluated in the glycerol etherification. The catalytic data reported in Fig. 12 show how the glycerol conversion rises as the reaction temperature increases from 50 % after 24 h at 210 ºC to 61% after 24 h at 240 ºC. Despite the higher conversion values with the temperature, the use of more severe conditions also causes uncontrolled etherification, as indicates the decrease of the diglycerol selectivity according as the temperature increases from 100% to 63% at 240 ºC due to an uncontrolled etherification forming undesired products, which are difficult to separate. Previous researches have pointed out that the products with low polymerization-degree, i.e. di- and tri-glycerols, have high industrial interest due to their wide range of uses and applications [13,27] while the formation of oligoglycerols due to larger polymerization are less interesting due to their physicochemical properties and the difficult to separate the mixture of compounds [62]. In addition, the use of higher temperature can favor the existence of undesired site reactions, which can generate toxic product such as acrolein or glycidol. Under the reaction conditions reported in the present study, these products have not been detected even [63,64]. In this sense, several authors [38,39,58,63] have established that the optimum reaction temperature to obtain diglycerols using solid basic catalyst between 200-220 ºC. This temperature does not provide the highest glycerol conversion; however, the side reactions are avoided, obtaining diglycerols as single product.

3.2.4. Kinetic test

The influence of the reaction time in the glycerol etherification for the mixed oxides with highest conversion values HTc-$Ni_{75\%}$ was evaluated along 24 h at 210 ºC using 2wt.% of catalyst (Fig. 13). The catalytic data show how both glycerol conversion and diglycerols selectivity increase as the reaction time does. It is noteworthy that the conversion value is very low in the early hours, reaching a glycerol conversion of only 10 % after 6 hours at 210 ºC. This fact suggests that it is necessary an activation step to favor the etherification since a diglycerols yield of 55% is reached after 24 h of reaction at 210 ºC. In this sense, several authors have proposed a mechanism where the glycerol etherification takes place in two steps. Firstly, the basic centers extract a $-H^+$ of the glycerol molecule and then an unsaturated site attacks the deprotonated glycerol to another glycerol molecule forming the diglycerol species [20,22]. Considering these data and those reported in the literature, it is expected that one of these steps of the reaction must be limited by the temperature.

Another key point in the use of heterogeneous catalysts is related to the leaching of the active phase. Previous investigations have pointed out that La, Cs or Mg-based catalysts supported on mesoporous silica suffer from the loss of active phase by leaching [63,65]. However, the concentration of Mg, Ni, Al and Zr in the reaction medium can be considered negligible [66], confirming the high stability of the mixed-oxides in the reaction medium.

3.2.5. Reuse of the catalysts

The reuse of the catalysts is a key parameter to attain sustainable and competitive catalysts. This study was carried out using 2 wt.% of HTc-$Ni_{75\%}$ catalyst at 220 ºC for 24 h. Between each run, the catalyst was separated by decantation and washed with H_2O. The catalytic data reveals that the glycerol conversion decrease from 55% to 35% after 4 runs. In all cases, the single product obtained in these reaction conditions was diglycerol.

The decrease of glycerol conversion could be ascribed to several parameters. As was indicated previously, the leaching of the Mg, Ni, Al or Zr can be considered as negligible [66] so the homogeneous contribution in the glycerol etherification should be discarded. The washing of the used catalyst with H_2O facilities the removal of the reagent and products strongly adsorbed. However, this washing can hydroxylate the mixed oxides in such a way the acid-based properties of the catalyst can be modified. The hydroxylation must cause a decrease of the acid and basic sites, which are involved in the glycerol etherification. Despite the decrease in catalytic activity after each run, washing with H_2O seems to be the most appropriate technique to reuse the catalyst since the separation by decantation results in a glycerol conversion of 21% while calcination gives rise to a conversion of a 37 % in the 2^{nd} run. This more pronounced decrease can be ascribed to the decantation is not enough to separate both reagents and producted, which interacts strongly with the mixed oxides species in such a way this active sites are partially blocked by subsequent runs. In the case the calcination method, the organic species adsorbed on the surface of the catalyst are removed by its decomposition at high temperature. This combustion process is an exothermic reaction so this treatment at high temperature can cause sintering of the catalyst, which is directly related with a decrease of the amount of available active sites.

4. Conclusions

A series of tetrametallic hydrotalcite with different Ni loading, were synthesized by coprecipitation method. Then, these hydrotalcites were calcined obtaining mixed-oxides with

low crystal size, being evaluated in the selective etherification of glycerol to yield mainly diglycerols. The catalytic data reveals that the incorporation of Ni species causes an increase of the acid and basic sites, which are directly related with the catalytic activity in the glycerol etherification.

The catalytic data show a highest glycerol conversion of 55%, with full selectivity towards diglycerols after 24 h of reaction at 210 ºC with only 2 wt.% of HTc-$Ni_{75\%}$ catalyst. The increase of the catalyst loading does not improve the catalytic behavior probably due to diffusional limitations. An increase of the reaction temperature favors the formation of triglycerols even tetraglycerols due to higher temperature leads to uncontrolled polymerization, obtaining products with a lower interest industry. Finally, the mixed oxides have shown high stability since the leaching is practically negligible.

Acknowledgements

The authors gratefully acknowledge support from Ministry of Economy and Competitiveness, Spain (Ministerio de Economía y Competitividad, España) through the project CTQ2015-68951-C3-3-R and FEDER. R.M.T. thanks to the Spanish Ministry of Economy and Competitiveness (IEDI-2016-00743) for the financial support within the I3 program. A special acknowledge to the Tunisian Ministry of Higher Education, Scientific Research, Information and Communication Technologies for the financial support.

REFERENCES

[1] Gholami Z, Abdullah AZ, Lee KT (2014) Dealing with the surplus of glycerol production from biodiesel industry through catalytic upgrading to polyglycerols and other value-added products. Renew Sust Energy Rev 39:327-341.

[2] Liang D, Gao J, Sun H, Chen P, Hou Z, Zheng X (2011) Selective oxidation of glycerol with oxygen in a base-free aqueous solution over MWNTs supported Pt catalysts. Appl Catal B 106:423-432.

[3] Nakagawa Y, Shinmi Y, Koso S, Tomishige K (2010) Direct hydrogenolysis of glycerol into 1,3-propanediol over rhenium-modified iridium catalyst. J Catal 272:191-194.

[4] Cecilia JA, García-Sancho C, Mérida-Robles JM, Santamaría-González J, Moreno-Tost R, Maireles-Torres P (2015) V and V-P containing Zr-SBA-15 catalysts for dehydration of glycerol to acrolein. Catal Today 254:43-52.

[5] García-Sancho C, Cecilia JA, Moreno-Ruiz A, Mérida-Robles JM, Santamaría-González J, Moreno-Tost R, Maireles-Torres P (2015) Influence of the niobium supported species on the catalytic dehydration of glycerol to acrolein. Appl Catal B 179:139-149.

[6] Valliyappan T, Bakhshi NN, Dalai AK (2008) Pyrolysis of glycerol for the production of hydrogen or syn gas, Pyrolysis of glycerol for the production of hydrogen or syn gas. Bioresource Technol 99:4476-4483.

[7] Pan S, Zheng L, Nie R, Xia S, Chen P, Hou Z (2012) Transesterification of glycerol with dimethyl carbonate to glycerol carbonate over Na–based zeolites. Chin J Catal 33:1772-1777.

[8] Pérez-Barrado E, Pujol MC, Aguiló M, Llorca J, Cesteros Y, Díaz F, Pallarès J, Marsal LF, Salagre P (2015) Influence of acid–base properties of calcined MgAl and CaAl layered double hydroxides on the catalytic glycerol etherification to short-chain polyglycerols. Chem Eng J 264:547-556.

[9] Wilms D, Stiriba SE, Frey H (2010) Hyperbranched polyglycerols: From the controlled synthesis of biocompatible polyether polyols to multipurpose applications Accounts Chem Res 43:129-141.

[10] Calderón M, Quadir MA, Sharma SK, Haag R (2010) Dendritic polyglycerols for biomedical applications. Adv Mater 22:190-218.

[11] Salehpour S, Dube MA (2011) Towards the sustainable production of higher-molecular-weight polyglycerol. Macromol Chem Phys 212:1284-1293.

[12] Yadav JD, Kulkarni PR, Vaidya KA, Shelke GT (2011) Niosomes: A review. J Pharm Res 4:632-636.

[13] Sivaiah MV, Robles-Manuel S, Valange S, Barrault J (2012) Recent developments in acid and base-catalyzed etherification of glycerol to polyglycerols. Catal Today 198:305-313.

[14] Zhou CH, Beltramini JN, Fan YX, Lu GQ (2008) Chemoselective catalytic conversion of glycerol as a biorenewable source to valuable commodity chemicals. Chem Soc Rev 37:527-549.

[15] Richter M, Krisnandi YK, Eckelt R, Martin A (2008) Homogeneously catalyzed batch reactor glycerol etherification by $CsHCO_3$. Catal Commun 9:2112-2116.

[16] Krisnandi YK, Eckelt R, Schneider M, Martin A, Richter M (2008) Glycerol upgrading over zeolites by batch-reactor liquid-phase oligomerization: heterogeneous versus homogeneous reaction. ChemSusChem 1:835-844.

[17] Medeiros MA, Araujo MH, Augusti R, de Oliveira LCA, Lago RMJ (2009) Acid-catalyzed oligomerization of glycerol investigated by electrospray ionization mass spectrometry. Braz Chem Soc 20:1667-1673.

[18] Harvey SB, Shen S (1996) One phase production of polyglycerol esters. Patent US 5585506 A.

[19] Lemke D, Nivens S (2007) Process for preparing polyglycerol and mixed ethers. Patent WO 2007/092407.

[20] Ruppert AM, Meeldijk JD, Kuipers BWM, Erné BH, Weckhuysen BM (2008) Glycerol etherification over highly active CaO-based materials: New mechanistic aspects and related colloidal particle formation. Chem Eur J 14:2016-2024.

[21] Ayoub M, Abdullah AZ (2013) LiOH-modified montmorillonite K-10 as catalyst for selective glycerol etherification to diglycerol. Catal Commun 34:22-25.

[22] Calatayud M, Ruppert AM, Weckhuysen BM (2009) Theoretical study on the role of surface basicity and Lewis acidity on the etherification of glycerol over alkaline earth metal oxides. Chem Eur J 15:10864-10870.

[23] González MD, Salagre P, Mokaya R, Cesteros Y (2014) Tuning the acidic and textural properties of ordered mesoporous silicas for their application as catalysts in the etherification of glycerol with isobutene. Catal Today 227:171-178.

[24] Cottin K, Clacens JM, Pouilloux Y, Barrault J (1998) Preparation of diglycerol and triglycerol by the direct polymerization of glycerol in the presence of the new solid catalysts. Ol Corps Gras Lipide 5:407-412.

[25] Richter M, Eckett R, Krisnandi YK, Martin A (2008) Verfahren zur selektiven herstellung von linearem diglycerin. Chem Ing Tech 80:1573-1577.

[26] Ayoub M, Abdullah AZ (2015) Diglycerol synthesis via solvent-free selective glycerol etherification process over lithium-modified clay catalyst. Chem Eng J 225:784-789.

[27] Sutter M, da Silva E, Duguet N, Raoul Y, Métay E, Lemaire M (2015) Glycerol ether synthesis: A bench test for green chemistry concepts and technologies. Chem Rev 115:8609-8651.

[28] Tichit D, Gérardin C, Durand R, Coq B (2006) Layered double hydroxides: precursors for multifunctional catalysts. Top Catal 39:89-96.

[29] Xu ZP, Zhang J, Adebajo MO, Zhang H, Zhou CH (2011) Catalytic applications of layered double hydroxides and derivatives. Appl Clay Sci 53:139-150.

[30] Roelofs JCAA, Lensveld DJ, van Dillen AJ, de Jong KP (2001) On the structure of activated hydrotalcites as solid base catalysts for liquid-phase aldol condensation. J Catal 203:184-191.

[31] Fan G, Li F, Evans DG, Duan X (2014) Catalytic applications of layered double hydroxides: recent advances and perspectives. Chem Soc Rev 43:7040-7066.

[32] Cerveny J, Splıchalova J, Kacer P, Kovanda F, Kuzma M, Cerveny L (2008) Molecular shape selectivity of hydrotalcite in mixed aldol condensations of aldehydes and ketones. J Mol Catal A 285:150-154.

[33] Abelló S, Medina F, Tichit D, Pérez-Ramírez J, Sueiras JE, Salagre P, Cesteros Y (2007) Aldol condensation of campholenic aldehyde and MEK over activated hydrotalcites. Appl Catal B. 70:577-584.

[34] Choudary BM, Kantam ML, Reddy CRV, Rao KK, Figueras F (1999) The first example of Michael addition catalysed by modified Mg–Al hydrotalcite. J Mol Catal A 146:279-284.

[35] Veloso CO, Pérez CN, de Souza BM, Lima EC, Dias AG, Monteiro JLF, Henriques CA (2008) Condensation of glyceraldehyde acetonide with ethyl acetoacetate over Mg,Al-mixed oxides derived from hydrotalcites. Micropor Mesopor Mater 107:23-30.

[36] Campos-Molina MJ, Santamaría-González J, Mérida-Robles J, Moreno-Tost R, Albuquerque MCG, Bruque-Gámez S, Rodríguez-Castellón E, Jiménez-López A, Maireles-Torres P (2010) Base catalysts derived from hydrocalumite for the transesterification of sunflower oil. Energy Fuels 24:979-984.

[37] Cantrell DG, Gillie LJ, Lee AF, Wilson K (2005) Structure-reactivity correlations in MgAl hydrotalcite catalysts for biodiesel synthesis. Appl Catal A 287:183-190.

[38] García-Sancho C, Moreno-Tost R, Mérida-Robles JM, Santamaría-González J, Jiménez-López A, Maireles Torres P (2011) Etherification of glycerol to polyglycerols over MgAl mixed oxides. Catal Today 167:84-90.

[39] Guerrero-Urbaneja P, García-Sancho C, Moreno-Tost R, Merida-Robles J, Santamaria-Gonzalez J, Jimenez-Lopez A, Maireles-Torres P (2014) Glycerol valorization by etherification to polyglycerols by using metal oxides derived from MgFe hydrotalcites. Appl Catal A 470:199-207.

[40] Wang J, Lei Z, Qin H, Zhang L, Li F (2011) Structure and catalytic property of Li-Al metal oxides from layered double hydroxide precursors prepared via a facile solution route. Ind Eng Chem Res 50:7120-7128.

[41] Kuhl S, Tarasov A, Zander S, Kasatkin I, Behrens M (2014) Cu-based catalyst resulting from a Cu, Zn, Al hydrotalcite-like compound: A microstructural, thermoanalytical, and in-situ XAS study. Chem Eur J 20:3782-3792.

[42] Gao P, Xie R, Wang H, Zhong L, Xia L, Zhang Z, Wei W, Sun Y (2015) Cu/Zn/Al/Zr catalysts via phase-pure hydrotalcite-like compounds for methanol synthesis from carbon dioxide. J. CO_2 Util 11:41-48.

[43] Velu S, Suzuki K, Okazaki M, Kapoor MP, Osaki T, Ohashi F (2000) Oxidative steam reforming of methanol over CuZnAl(Zr)-Oxide catalysts for the selective production of hydrogen for fuel cells: Catalyst characterization and performance evaluation. J Catal 194:373-384.

[44] Brunauer S, Emmett PH, Teller E (1938) Adsorption of gases in multimolecular layers. J Am Chem Soc 60:309-319.

[45] Landers J, Gor GY, Neimark AV (2013) Density functional theory methods for characterization of porous materials. Colloid Surf. A 437:3-32.

[46] Aramendia MA, Avilés Y, Benitez JA, Borau V, Jiménez C, Marinas JM, Ruiz JR, Urbano FJ 1999. Comparative study of Mg/Al and Mg/Ga layered double hydroxides. Micropor Mesopor Mater 29 :319-328.

[47] Noda Pérez C, Pérez CA, Henriques CA, Monteiro JLF (2004) Hydrotalcites as precursors for Mg,Al-mixed oxides used as catalysts on the aldol condensation of citral with acetone. Appl Catal A 272:229-240.

[48] Thommes M, Kaneko K, Neimark AV, Olivier JP, Rodriguez-Reinoso F, Rouquerol J, Sing KSW (2015) Physisorption of gases, with special reference to the evaluation of surface area and pore size distribution (IUPAC Technical Report). Pure Appl Chem 87:1051-1069.

[49] Dębek R, Motak M, Duraczyska D, Launay F, Gálvez ME, Grzybek T, da Costa P (2016) Methane dry reforming over hydrotalcite-derived Ni–Mg–Al mixed oxides: The influence of Ni content on catalytic activity, selectivity and stability. Catal Sci Technol 6:6705-6715.

[50] Sundaramurthy, V, Dalai AK, Djaye JA (2008) The effect of phosphorus on hydrotreating property of NiMo/γ-Al_2O_3 nitride catalyst- Appl Catal A 335:204-210.

[51] Shen J, Tu M, Hu C (1998) Structural and surface acid/base properties of hydrotalcite-derived MgAlO oxides calcined at varying temperatures. J Solid State Chem 137:295-301.

[52] Lino AVP, Assaf EM, Assaf JM (2016) Hydrotalcites derived catalysts for syngas production from biogas reforming: Effect of nickel and cerium load. Catal Today 289:78-88.

[53] García-Sancho C, Moreno-Tost R, Mérida-Robles J, Santamaría-González J, Jiménez-Lopez A, Maireles-Torres P (2012) Zirconium doped mesoporous silica catalysts for dehydration of glycerol to high added-value products. Appl Catal A 433:179-187.

[54] Cecilia JA, García-Sancho C, Mérida-Robles JM, Santamaría-González J, Infantes-Molina A, Moreno-Tost R, Maireles-Torres P (2017) Aluminum doped mesoporous silica SBA-15 for glycerol dehydration to value-added chemicals. J Sol-Gel Sci Technol 83:342-354.

[55] Patrono P, La Ginestra A, Ramis G, Busca G (1994) Conversion of 1-butene over WO_3-TiO_2 catalysts. Appl Catal A 107:249-266.

[56] Cecilia, JA, García-Sancho C, Franco F (2013) Montmorillonite based porous clay heterostructures: Influence of Zr in the structure and acidic properties. Micropor Mesopor Mater 176:95-102.

[57] Solsona B, Concepción P, López Nieto JM, Dejoz A, Cecilia JA, Agouram S, Soriano M D, Torres V, Jiménez-Jiménez J, Rodríguez Castellón, E (2016) Nickel oxide supported on porous clay heterostructures as selective catalysts for the oxidative dehydrogenation of ethane. Catal Sci Technol 6:3419-3429.

[58] Barros, FJS, Moreno-Tost R, Cecilia JA, Ledesma-Muñoz AL, de Oliveira LCC, Luna FMT, Vieira RS (2017) Glycerol oligomers production by etherification using calcined eggshell as catalyst. Molec. Catal. 433:282-290.

[59] Correia LM, Campelo NS, Novaes DS, Cavalcante CL, Cecilia JA, Rodríguez-Castellón E, Vieira R.S (2015) Characterization and application of dolomite as catalytic precursor for canola and sunflower oils for biodiesel production. Chem Eng J 269:35-43.

[60] Liu P, Derchi M, Hensen EJM (2014) Promotional effect of transition metal doping on the basicity and activity of calcined hydrotalcite catalysts for glycerol carbonate synthesis. Appl Catal B144:135-143.

[61] Clacens JM, Pouilloux Y, Barrault J, Linares C, Goldwasser M (1998) Mesoporous basic catalysts: comparison with alkaline exchange zeolites (basicity and porosity). Application to the selective etherification of glycerol to polyglycerols. Stud Surf Sci Catal 118:895-902.

[62] Martin A, Richter M (2011) Oligomerization of glycerol a critical review. Eur J Lipid Sci Technol 113:100-17.

[63] Gholami Z, Abdullah AZ, Lee KT (2014) Heterogeneously catalyzed etherification of glycerol to diglycerol over calcium-lanthanum oxide supported on MCM-41: A heterogeneous basic catalyst. Appl Catal A 479:76-86.

[64] Ayoub M, Khayoon MS, Abdullah AZ (2012) Synthesis of oxygenated fuel additives via the solventless etherification of glycerol. Bioresource Technol 112:308-312.

[65] Clacens JM, Pouilloux Y, Barrault J (2002) Selective etherification of glycerol to polyglycerols over impregnated basic MCM-41 type mesoporous catalysts. Appl Catal A 227:181-190.

[66] Barros FJS,·Cecilia JA, Moreno-Tost R,· de Oliveira MF, Rodríguez-Castellón E, Luna FMT, Vieira RS (2018) Glycerol oligomerization using low cost dolomite catalyst. Waste and Biomass Valorization. In press: https://doi.org/10.1007/s12649-018-0477-5